Clinical Cancer Research

HER2 Reactivation through Acquisition of the HER2 L755S Mutation as a Mechanism of Acquired Resistance to HER2-targeted Therapy in HER2+ Breast Cancer

Xiaowei Xu[1,2,3], Carmine De Angelis[1,2], Kathleen A. Burke[4], Agostina Nardone[1,2], Huizhong Hu[1,2], Lanfang Qin[1,2], Jamunarani Veeraraghavan[1,2], Vidyalakshmi Sethunath[1,2,3], Laura M. Heiser[5], Nicholas Wang[5], Charlotte K.Y. Ng[4], Edward S. Chen[2,6], Alexander Renwick[2,6], Tao Wang[1,2], Sarmistha Nanda[1,2], Martin Shea[1,2], Tamika Mitchell[1,2], Mahitha Rajendran[1,2], Ian Waters[7], Daniel J. Zabransky[7], Kenneth L. Scott[6], Carolina Gutierrez[1,2], Chandandeep Nagi[1,2], Felipe C. Geyer[4], Gary C. Chamness[1,2], Ben H. Park[7], Chad A. Shaw[2,6], Susan G. Hilsenbeck[1,2], Mothaffar F. Rimawi[1,2], Joe W. Gray[5], Britta Weigelt[4], Jorge S. Reis-Filho[4], C. Kent Osborne[1,2,8,9], and Rachel Schiff[1,2,8,9]

Abstract

Purpose: Resistance to anti-HER2 therapies in HER2+ breast cancer can occur through activation of alternative survival pathways or reactivation of the HER signaling network. Here we employed BT474 parental and treatment-resistant cell line models to investigate a mechanism by which HER2+ breast cancer can reactivate the HER network under potent HER2-targeted therapies.

Experimental Design: Resistant derivatives to lapatinib (L), trastuzumab (T), or the combination (LR/TR/LTR) were developed independently from two independent estrogen receptor ER+/HER2+ BT474 cell lines (AZ/ATCC). Two derivatives resistant to the lapatinib-containing regimens (BT474/AZ-LR and BT474/ATCC-LTR lines) that showed HER2 reactivation at the time of resistance were subjected to massive parallel sequencing and compared with parental lines. Ectopic expression and mutant-specific siRNA interference were applied to analyze the mutation functionally. *In vitro* and *in vivo* experiments were performed to test alternative therapies for mutant HER2 inhibition.

Results: Genomic analyses revealed that the *HER2*L755S mutation was the only common somatic mutation gained in the BT474/AZ-LR and BT474/ATCC-LTR lines. Ectopic expression of *HER2*L755S induced acquired lapatinib resistance in the BT474/AZ, SK-BR-3, and AU565 parental cell lines. *HER2*L755S-specific siRNA knockdown reversed the resistance in BT474/AZ-LR and BT474/ATCC-LTR lines. The HER1/2–irreversible inhibitors afatinib and neratinib substantially inhibited both resistant cell growth and the HER2 and downstream AKT/MAPK signaling driven by *HER2*L755S *in vitro* and *in vivo*.

Conclusions: HER2 reactivation through acquisition of the *HER2*L755S mutation was identified as a mechanism of acquired resistance to lapatinib-containing HER2-targeted therapy in preclinical HER2-amplified breast cancer models, which can be overcome by irreversible HER1/2 inhibitors. *Clin Cancer Res; 23(17); 5123–34. ©2017 AACR.*

[1]Lester & Sue Smith Breast Center, Baylor College of Medicine, Houston, Texas. [2]Dan L. Duncan Comprehensive Cancer Center, Baylor College of Medicine, Houston, Texas. [3]Department of Biochemistry and Molecular Biology, Baylor College of Medicine, Houston, Texas. [4]Department of Pathology, Memorial Sloan Kettering Cancer Center, New York, New York. [5]Department of Biomedical Engineering and Oregon Center for Spatial Systems Biomedicine, Oregon Health & Science University, Portland, Oregon. [6]Department of Molecular & Human Genetics, Baylor College of Medicine, Houston, Texas. [7]Sidney Kimmel Comprehensive Cancer Center at Johns Hopkins, Baltimore, Maryland. [8]Department of Medicine, Baylor College of Medicine, Houston, Texas. [9]Department of Molecular and Cellular Biology, Baylor College of Medicine, Houston, Texas.

Xu et al.

Translational Relevance

Despite the efficacy of first-generation HER2-targeted therapy, such as trastuzumab and lapatinib, in HER2$^+$ breast cancer, acquired resistance to these drugs, alone or in combination, frequently occurs in patients. HER2 pathway reactivation by the *HER2*L755S mutation was found to constitute a mechanism of acquired resistance to lapatinib-containing HER2-targeted therapies in HER2$^+$ breast cancer models. This mutation also conferred resistance to the dual HER2 blockade trastuzumab + pertuzumab and less sensitivity to the antibody–drug conjugate trastuzumab emtansine (T-DM1). Our findings support the contention that second-generation irreversible HER1/2 inhibitors, such as afatinib and neratinib, may offer therapeutic approaches for HER2$^+$ breast cancer patients whose tumors harbor the *HER2*L755S mutation.

Introduction

The *HER2* gene is amplified and/or overexpressed in about 15% of breast cancers, which clinically defines the HER2$^+$ breast cancer subtype. HER2 overexpression has been shown to result in activation of downstream AKT and MAPK signaling through either homo- or heterodimerization with other HER family members. HER2$^+$ breast cancers have higher proliferation rates and have been shown to be associated with poorer prognosis prior to the advent of HER2-targeted treatments (1). Currently, the FDA-approved HER2-targeted therapies include the mAbs trastuzumab (T) and pertuzumab (P), the small-molecule HER1/2 tyrosine kinase inhibitor (TKI) lapatinib (L), and the antibody–drug conjugate trastuzumab emtansine (T-DM1), all of which have greatly improved the outcome of HER2$^+$ breast cancer patients (2–7). Our group and others have shown that anti-HER2 drug combinations, such as lapatinib + trastuzumab, can more completely block the HER receptor layer than each single agent alone, and, thereby, achieve tumor regression and eradication in preclinical models (8–10). In the NeoALTTO trial, the lapatinib + trastuzumab combination therapy showed superior effect over lapatinib or trastuzumab therapy alone when combined with chemotherapy (11). In our 12-week neoadjuvant lapatinib + trastuzumab trial (TBCRC006/NCT00548184) in patients with stages II and III BK;HER2$^+$ breast cancer, a high pathologic complete response (pCR) rate (27%) was achieved with the lapatinib + trastuzumab combination even without the addition of chemotherapy (8, 9, 11, 12). Despite the benefit of HER2-targeted therapy, *de novo* and acquired resistance to lapatinib, trastuzumab, or the combination commonly occurs (12–15).

We and others have shown that acquired resistance to anti-HER2 therapies is a convergent phenotype (15). Resistance can occur through a multitude of mechanisms that result in HER pathway reactivation (15) or activation of alternative survival pathways, such as upregulation of ER signaling (10), upregulation of the PI3K pathway via PIK3CA mutations or reduced PTEN expression (16–18), and upregulation of β1-integrin signaling (19). Therefore, germane to the development of fit-for-purpose biomarkers and optimal alternative therapies for HER2$^+$ breast cancer patients is the elucidation of resistance mechanisms predicting resistance to lapatinib, trastuzumab, and combination of anti-HER treatments.

Recent massive parallel sequencing studies have revealed that HER2 can drive breast cancer growth not only by amplification in HER2$^+$ breast cancer but also through HER2-activating mutations preferentially in breast cancers lacking HER2 overexpression and/or gene amplification (20, 21). *HER2* mutations occur in about approximately 3% of breast cancer patients, among which the *HER2*L755S mutation is the most common [results based on the Cancer Genome Atlas Study (TCGA; cBioPortal); 22, 23]. This mutation has been associated with lapatinib resistance when overexpressed in HER2$^-$ cells (20, 24, 25). Yet it is not clear whether it is an activating mutation (20), and little is known about its role in activating HER2 and driving acquired resistance to HER2-targeted therapies in HER2$^+$ breast cancer. Here we demonstrate that the *HER2*L755S mutation, which was detected in the BT474/AZ-LR and BT474/ATCC-LTR lines, can induce resistance to potent anti-HER2 therapies by reactivating HER2 signaling in HER2$^+$ breast cancer models. This resistance can be pharmacologically overcome by irreversible dual HER1/2 inhibitors. Treatment of HER2$^+$ breast cancer patients harboring activating lapatinib-resistant *HER2* mutations, such as the L755S mutation, with irreversible HER1/2 inhibitors may improve their clinical outcome.

Materials and Methods

Chemicals

Lapatinib and trastuzumab were purchased from LC Laboratories and Mckesson Specialty Health, respectively. Stocks of lapatinib and trastuzumab were prepared as described previously (10, 19). Afatinib and neratinib were purchased from LC Laboratories and Selleck Chemicals, respectively. Stocks of afatinib and neratinib were prepared with DMSO.

Cell lines

Source, culture medium, and conditions of the BT474/AZ parental (P), SK-BR-3, and AU565 lines were described previously (10). The BT474/ATCC-P line was purchased from ATCC and cultured in the same medium and conditions as the BT474/AZ-P line. Resistant (R) derivatives of both BT474-P lines to HER2-targeted therapies were derived independently: cells were treated with gradually increasing doses until they resumed growth in the presence of 1 µmol/L lapatinib (LR), 50 µg/mL trastuzumab (TR), or the combination (lapatinib and trastuzumab; LTR) as previously described (Supplementary Table S1; ref. 10). All cell lines were authenticated at the MD Anderson Characterized Cell Line Core Facility within 6 months of performing the experiments. All cell lines were tested to be mycoplasma-free by MycoAlert Mycoplasma Detection Kit (Lonza).

Whole-exome sequencing

Cell line genomic DNA (gDNA) was isolated using the Wizard Genomic DNA Kit (Promega). Exome libraries of the BT474/AZ-P, BT474/AZ-LR, BT474/ATCC-P, and BT474/ATCC-LTR cell line genomic DNA were generated using the Agilent SureSelect XT kit and Agilent Automation Systems NGS system per the manufacturer's instructions. Paired-end 101-bp sequencing was performed on an Illumina HiSeq 2000 sequencer, achieving a median coverage of 52.96× (range 21.22–91.96×; Supplementary Table S2). Sequence reads have

been deposited to the NCBI Sequence Read Archive under the accession SRP076305.

Paired-end whole-exome sequencing reads were aligned to the human reference genome GRCh37 using the Burrow-Wheeler Aligner (26). Local realignment, duplicate removal, and quality score recalibration were performed using the Genome Analysis Toolkit (GATK; ref. 27). Mutations in the derivative cell lines that were not detected in the BT474/ATCC parental cell line (BT474/ATCC-P) were defined using MuTect (28) for the single nucleotide variants, and a combination of Strelka and Varscan2 (29, 30) for insertions and deletions, with the BT474/ATCC-P line as the reference. SNVs and indels with mutant allelic fraction of less than 1% and/or supported by fewer than 5 reads were disregarded (31). Variants found with >5% global minor allele frequency in dbSNP (Build 137) or that were covered by <10 reads in the tumor or <5 reads in the BT474/ATCC-P cell line were disregarded. Variants for which the tumor variant allele fraction was <5 times than that of the variant allele fraction found in the BT474/ATCC-P cell line were disregarded. The cancer cell fraction (CCF) of each mutation was inferred using ABSOLUTE (v1.0.6; ref. 32) and mutations were classified according to pathogenicity (details see Supplementary Methods).

Single-nucleotide polymorphism array

Single-nucleotide polymorphism (SNP) array analysis of the BT474/AZ-P, BT474/AZ-LR, BT474/ATCC-P, and BT474/ATCC-LTR cell lines was performed with the Human Omni2.5-8 Bead-Chip Kit (Illumina) following the manufacturer's instructions. Log$_2$ ratios and B-allele frequencies were exported from GenomeStudio. Allele-specific copy number alterations were estimated using ASCAT (33) as previously described. SNP array data have been deposited to the NCBI Gene Expression Omnibus under the accession GSE83608.

RNA sequencing

Total RNA of the BT474/AZ-P, BT474/AZ-LR, BT474/ATCC-P, and BT474/ATCC-LTR cell lines was extracted with RNeasy Mini Kit (Qiagen). The RNA-seq libraries of these lines were prepared using the TruSeq RNA Sample Preparation Kit (Illumina) and the Agilent Automation NGS system per manufacturers' instructions. Samples were sequenced on an Illumina HiSeq platform with paired-end 100-bp reads.

For the analysis of the expression of novel mutations (i.e., found in the BT474 derivative cell lines but not in the BT474/ATCC-P cell line), paired-end sequence reads aligned using Tophat (34) were interrogated from pileup files generated using Samtools (35) from the aligned RNA sequencing data. Mutations with MAF of at least 0.01% in the RNA sequencing data were considered to be expressed. The expression of the HER2L755S mutation was visualized using the Integrative Genomics Viewer (IGV; ref. 36). Sequence reads have been deposited to the NCBI Sequence Read Archive under the accession number SRP076300.

Ectopic expression of wild-type and mutant HER2

HA-tagged WT-, G572V-, L755S-, and G572V/L755S-HER2 were expressed in the BT474/AZ-P line using a doxycycline-inducible lentiviral system (37). Wild-type (WT) and HER2L755S were also expressed in SK-BR-3 and AU565 lines. Mutant HER2 cDNA

constructs were generated through site-directed mutagenesis (Stratagene). Primers used for the mutagenesis were:

G572V-forward (F): GTGTCAGCCCCAGAATGTCTCAGTGACC TGTTTTG;
G572V-reverse (R): CAAAACAGGTCACTGAGACATTCTGGGG CTGACAC;
L755S-F: GTGGCCATCAAAGTGTCGAGGGAAAACACATCC;
L755S-R: GGATGTGTTTTCCCTCGACACTTTGATGGCCAC.

WT and mutant HER2 cDNA were shuffled into doxycycline-inducible pHAGE-Ubc-DEST-HA expression plasmids (from Dr. Thomas Westbrook, Baylor College of Medicine, Houston, TX; ref. 37). Lentiviral supernatants were generated by transient transfection of 293T cells using TransIT 293 transfection reagent (Mirus Bio LLC) and harvested 48 hours posttransfection. BT474/AZ-P cells were infected with lentiviral supernatant and selected with 800 µg/mL Geneticin (Invitrogen) 48 hours after infection. Transduced cell lines (BT474/AZ-P-WT, BT474/AZ-P-G572V, BT474/AZ-P-L755S, and BT474/AZ-P-G572V/L755S) as well as the transduced SK-BR-3 and AU565 lines were further selected with 1 µg/mL doxycycline + 1 µmol/L L for 3–5 weeks (or, where indicated, continuously) as described previously (38).

Mutant-specific RNA interference

siRNAs were designed to selectively knock down the HER2L755S mutation (C>T mismatch was placed at position 16 (Seq1) or position 17 (Seq2) of the 19mer siRNA (39)): Seq1: 5′-UGGCCAUCAAAGUGUCGAGdTdT-3′, Seq2: 5′-GUGGCCA-UCAAAGUGUCGAdTdT-3′ (Sigma). The nontargeting control (Ctrl) siRNA sequence was: 5′-UUCUCCGAACGUGUCAC-GUdTdT-3′ (40). Five-thousand cells per well of the BT474 parental or resistant lines were plated in 96-well plates in six replicates for siRNA transfection (zero day). Cells were transfected with transfection reagent alone (mock), Ctrl siRNA, or HER2L755S-specific siRNAs by reverse transfection using RNAi-MAX Lipofectamine per manufacturer's instructions (Invitrogen). Medium was replaced the next day with original treatments of each line. Cell growth was assessed 7 days after transfection by cell growth assay (10).

Cell growth assay

Five-thousand cells per well of the BT474/AZ-P, BT474/AZ-LR, BT474/AZ-LTR, BT474/ATCC-P, BT474/ATCC-LTR cells were plated in 96-well plates in quadruplicate to measure the drug response or siRNA interference effect (zero days). Medium was replaced the next day with regular medium or drug-containing medium, and replaced again at 4 days. Cell growth was assessed at six days by methylene blue assay as described previously (10). Relative growth percentage was determined by [(O.D. 655 nm at 6 days − O.D. 655 nm at zero days) Treatment]/[(O.D. 655 nm at 6 days − O.D. 655 nm at zero days) Control], as described previously (10).

Immunoblotting assay

Protein lysates were extracted as described previously (10). Twenty micrograms of each protein sample were separated by electrophoresis on NuPAGE Novex 4%–12% Bis-Tris Gels (Invitrogen) and transferred by electroblotting onto nitrocellulose membranes using the iBlot 2 Dry Blotting System (Invitrogen). Blots were blocked with 5% milk for 1 hour and then reacted at 4°C overnight with respective primary antibodies (see Supplementary Methods) diluted in 5% BSA + 0.05% Tween-20 at

dilutions as per manufacturer's directions. Blots were washed 3 times in PBS with 0.05% Tween-20 (PBST) and then incubated with matching HRP-linked secondary antibody (Cell Signaling Technology) diluted in 5% BSA + 0.05% Tween-20 at 1:2,000 dilutions for 1 hour. The blots were then washed three times with PBST, visualized by chemiluminescence on a ChemiDoc Touch Imaging System, and analyzed using the Image Lab Software Version 5.2.1 (Bio-Rad). Experiments were repeated at least twice. For details of immunoblotting, see Supplementary Methods.

Xenograft studies

BT474/AZ-LR cells were maintained as described previously (10). Animal care was in accordance with institutional guidelines. Ovariectomized 5- to 6-week-old athymic mice (Harlan Sprague Dawley) supplemented with estrogen pellets (E2; ref. 41) received subcutaneous injection of 5×10^6 BT474/AZ-LR cells (ER$^+$/HER2$^+$) as described previously (8). Starting the next day, mice were treated with 100 mg/kg lapatinib once daily orally, 7 days/week. After two weeks, 16 mice bearing xenografts that reached approximately 150 mm^3 were randomized to 2 treatment groups (8 mice/group): continued lapatinib (E2 + lapatinib, 100 mg/kg once daily orally, 7 days/week) or switched to afatinib (E2 + afatinib, 20 mg/kg once daily orally, 7 days/week). The rest of the mice remained on E2 + lapatinib treatment until tumors reached approximately 350 mm^3 and were then randomized to 3 groups (12 mice/group): estrogen deprivation by removal of estrogen pellets (ED) plus vehicle (0.5% hydroxypropyl-methylcellulose, 0.1% Tween 80) (ED + Veh), ED + lapatinib, or ED + afatinib. Tumor volumes were measured twice per week as described previously (8, 10, 42). Mice were sacrificed and tumors were harvested when the tumors reached 1,000 mm^3 or at completion of the experiment (day 16 for E2 arms and day 85 for ED arms except for mice which reached complete tumor eradication). Each tumor analyzed was from a different mouse; tumor tissue was harvested from each individual mouse and preserved in liquid nitrogen or formalin-fixed and paraffin embedded (FFPE) for later analyses.

IHC

BT474 tumor xenografts were excised and tumor slices were immediately placed into formalin and fixed overnight. The next day, fixed tissue slices were washed with 70% ethanol before processing and paraffin embedding. IHC was performed as described previously (10) using the same primary antibodies against phospho proteins as in the Western blots.

Statistical analyses

For the L755S mutant–silencing experiment, data analyses were performed for BT474/AZ and BT474/ATCC models separately. Cell growth was compared using a general linear model with cell lines (parental/resistant derivative), treatment (siRNA transfected/mock, drug treatments/DMSO), and their interaction. Results from two independent experiments were combined for analysis and each experiment was considered a categorical blocking factor. For purposes of plotting, model-estimated group means and 95% confidence limits were used. Plots show data from two experiments combined. For the drug response experiments, IC$_{50}$ values were generated through GraphPad Prism (version 6.05) using the log (inhibitor) versus response-variable slope model (GraphPad).

For the xenograft experiment, Kaplan–Meier survival plots were generated from survival analysis performed for progression (tumor size tripling/doubling from day of randomization in the E2/ED treatment groups, respectively), and regression (tumor size halving from day of randomization). Time to doubling/tripling was estimated by linear interpolation. Complete response was defined as complete tumor disappearance for at least 3 consecutive weeks and complete response rates were calculated on the basis of the total number of animals treated in each group. Tumor size halving required two consecutive observations of the regression; time to regression was defined by the second observation time. If the tumor size had not reached an event threshold by the last observation, then it was considered as censored at the last time point. Difference of time to tumor progression/regression between groups was analyzed by generalized Wilcoxon test and pairwise comparison with P value adjustment using simulated method. Differences of IHC H-score, relative expression of HER2L755S and total HER2 RNA, and relative cell growth and colony formation upon drug treatments were compared using one-way ANOVA.

Results

The HER2L755S mutation is associated with acquired resistance to lapatinib-containing regimens and reactivates HER2 signaling in BT474 models

As previously described by our group, the BT474/AZ cell line is a subline of the BT474/ATCC cell line that can be effectively grown *in vivo* as xenografts (10). Both BT474 models are ER$^+$/HER2$^+$ and harbor HER2 gene amplification. We have previously shown that in the BT474/AZ cell model, during the development of lapatinib resistance, HER2 signaling was inhibited at the early stage and then reactivated after prolonged lapatinib treatment [BT474/AZ-late LR as described previously (10), hereafter termed the BT474/AZ-LR line; Fig. 1A and Supplementary Fig. S1A]. HER2 signaling was not reactivated in the BT474/AZ-LTR derivative (Supplementary Fig. S1A), or in derivatives resistant to lapatinib-containing regimens of five additional HER2$^+$ breast cancer cell models (HCC202, AU565, MDA-MB-361, UACC812, and HCC1954) we have previously described (10, 19). Here we focused on the phenomenon of HER2 reactivation in the lapatinib-containing regimen as it has been previously shown that lapatinib has a stronger inhibitory effect on HER2 kinase activity than T (43, 44). To understand whether HER2 reactivation during lapatinib resistance is found only in the specific BT474/AZ subline of the BT474 cell model, we next investigated its parental line BT474/ATCC. Importantly, in the BT474/ATCC model, we also found HER2 and its downstream signaling to be reactivated in its LT-resistant derivative (BT474/ATCC-LTR line; Fig. 1A; Supplementary Fig. S1A) but not in the LR derivative. Therefore, we observed HER2 reactivation in certain derivatives resistant to lapatinib-containing regimens in both the BT474/AZ (LR) and BT474/ATCC (LTR) models.

Previously we have shown that HER2 knockdown can significantly inhibit growth of the BT474/AZ-LR line, suggesting that the resistant growth of this line is dependent on the reactivated HER2 signaling in the presence of HER2-targeted therapy (10). HER2 activating mutations have been shown to be associated with resistance to lapatinib in HER2-negative breast cancer (20). Therefore, we hypothesized that HER2 reactivation in the two HER2$^+$ BT474-resistant lines could result from HER2-activating
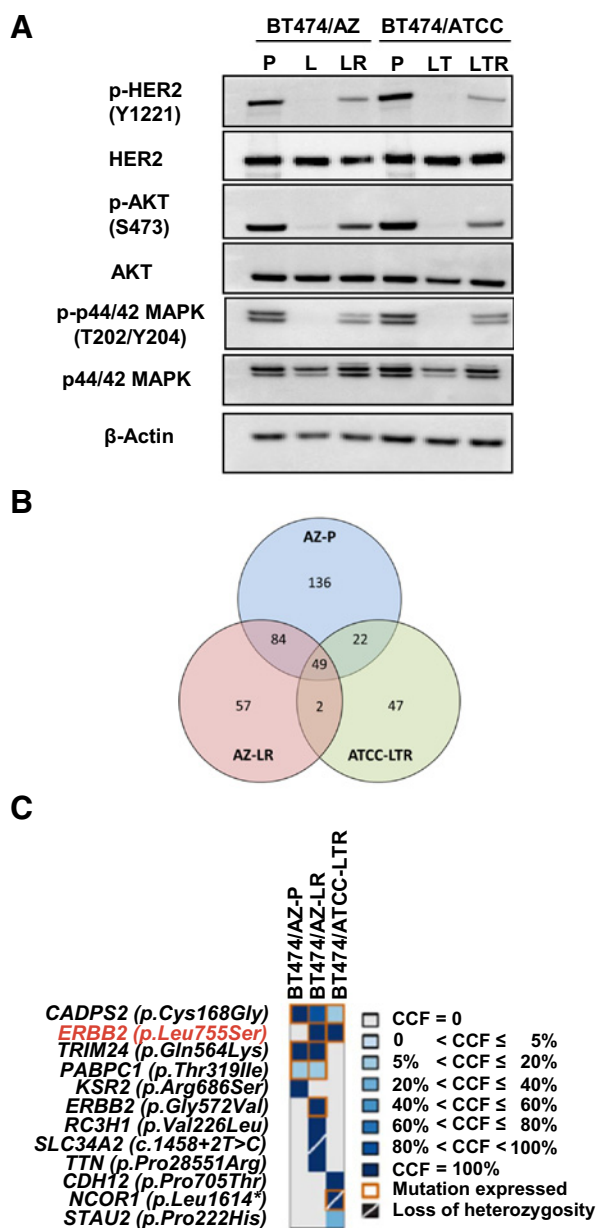
Figure 1.
The *HER2*L755S mutation reactivates HER2 signaling in BT474 models and is associated with acquired resistance to lapatinib (L)-containing regimens. **A,** Western blot analyses of lapatinib/lapatinib + trastuzumab (LT)-treated BT474 parental and resistant cells. BT474/AZ-P were treated for 6 hours with DMSO or 1 μmol/L lapatinib. BT474/ATCC-P cells were treated with DMSO or 1 μmol/L lapatinib + 10 μg/mL trastuzumab (T). BT474/AZ-LR cells were cultured in the presence of 1 μmol/L lapatinib and BT474/ATCC-LTR cells were cultured in the presence of 1 μmol/L L + 10 μg/mL trastuzumab. **B,** Number of mutations detected using whole-exome sequencing identified in single samples or multiple samples in the BT474/AZ-P, BT474/AZ-LR, and BT474/ATCC-LTR lines using the BT474/ATCC-P line as reference. **C,** Pathogenic mutations identified by whole-exome sequencing (Supplementary Methods) in the BT474/AZ-P, BT474/AZ-LR, and BT474/ATCC-LTR lines using the BT474/ATCC-P line as reference are shown. The shade of blue in each block represents the cancer cell fraction (CCF) of each mutation in each line. Orange squares represent mutations that were found to be expressed using RNA sequencing. Mutations associated with the loss of the wild-type allele are indicated by a diagonal bar. The *HER2* (encoded by the gene *ERBB2*) L755S mutation is highlighted in red.

mutations. To test this, we subjected both BT474 parental lines (BT474/AZ-P and BT474/ATCC-P) and their two HER2-reactivated lapatinib-resistant derivatives (BT474/AZ-LR and BT474/ATCC-LTR) to whole-exome sequencing and RNA sequencing (Supplementary Table S3). Using the BT474/ATCC-P line as reference for mutation calling (i.e., the sequencing results of the BT474/ATCC-P cells were used as the "germline" reference for the analysis of the resistant models), we identified a *HER2* mutation (L755S) that was present in both lapatinib-resistant cell line derivatives but was absent in the BT474/ATCC-P line (Fig. 1B; Supplementary Fig. S1B). Importantly, the *HER2*L755S mutation was identified as the only pathogenic mutation shared by the two resistant lines, but not present in the BT474/AZ-P line (Fig. 1C; Supplementary Fig. S1B). Furthermore, analysis of the CCF of the mutations using ABSOLUTE (32) revealed that the *HER2*L755S mutation was clonally present in the two BT474-resistant lines (i.e., bioinformatically inferred to be present in virtually all cells, Fig. 1C). Using digital PCR, we could confirm the presence of this mutation in BT474/AZ-LR and BT474/ATCC-LTR, but not in the BT474/AZ-P and BT474/ATCC-P cells at the sensitivity of 1/10,000 (Supplementary Fig. S1H). In addition, cDNA Sanger sequencing also confirmed that the *HER2*L755S mutation was clonally expressed only in the two HER-reactivated LR/LTR lines (BT474/AZ-LR and BT474/ATCC-LTR; Supplementary Table S3) but not in the BT474 parental lines, BT474/AZ-LTR and TR, BT474/ATCC-LR and TR derivative lines (Supplementary Fig. S1B–S1D, S1F, and S1G). Additional sequencing also confirmed that the *HER2*L755S mutation was present only in the two HER-reactivated LR/LTR lines of BT474 model, but not in any of the derivatives resistant to lapatinib-containing regimens of five additional HER2+ breast cancer cell models mentioned above (10, 19).

Apart from the L755S mutation, whole-exome and RNA sequencing of BT474 and its derivative cell line models identified a second *HER2* mutation (G572V), which was in the BT474/AZ-LR but not in the BT474/AZ-P, BT474/ATCC-P, BT474/ATCC-LTR, BT474/AZ-LTR, BT474/ATCC-LR, BT474/AZ-TR, or BT474/ATCC-TR derivative lines (Supplementary Table S3; Supplementary Fig. S1B and S1E). There have been no reports of the *HER2*G572V mutation in cell line or clinical sequencing data. Given that the L755S but not the G572V mutation was found to be shared by the two resistant lines, we hypothesized that the *HER2*L755S mutation but not the G572V mutation may reactivate HER2 signaling and drive resistance to HER2-targeted therapies in the BT474/AZ-LR and BT474/ATCC-LTR lines.

The *HER2*L755S mutation is the driver of acquired resistance in the two BT474 L/LT–resistant derivatives with HER2 reactivation

To investigate whether the *HER2*L755S mutation can induce lapatinib resistance in the HER2+ breast cancer preclinical models and test whether the *HER2*G572V mutation has any function in inducing lapatinib resistance, we ectopically expressed HA-tagged WT-, G572V-, L755S-, and G572V/L755S-*HER2* in the BT474/AZ-P cells. Expression of the doxycycline-inducible HA-tagged *HER2* constructs was verified by Western blot analysis (Fig. 2A). To avoid the effect of the overexpressed endogenous WT *HER2*, we selected the exogenous-*HER2* expressing cells with doxycycline + lapatinib for 5 weeks. After 5 weeks of selection, only the L755S *HER2*- and G572/L755S *HER2*–expressing cells, but not the WT *HER2*- and G572V-*HER2*–expressing cells, survived the selection (Fig.

Xu et al.
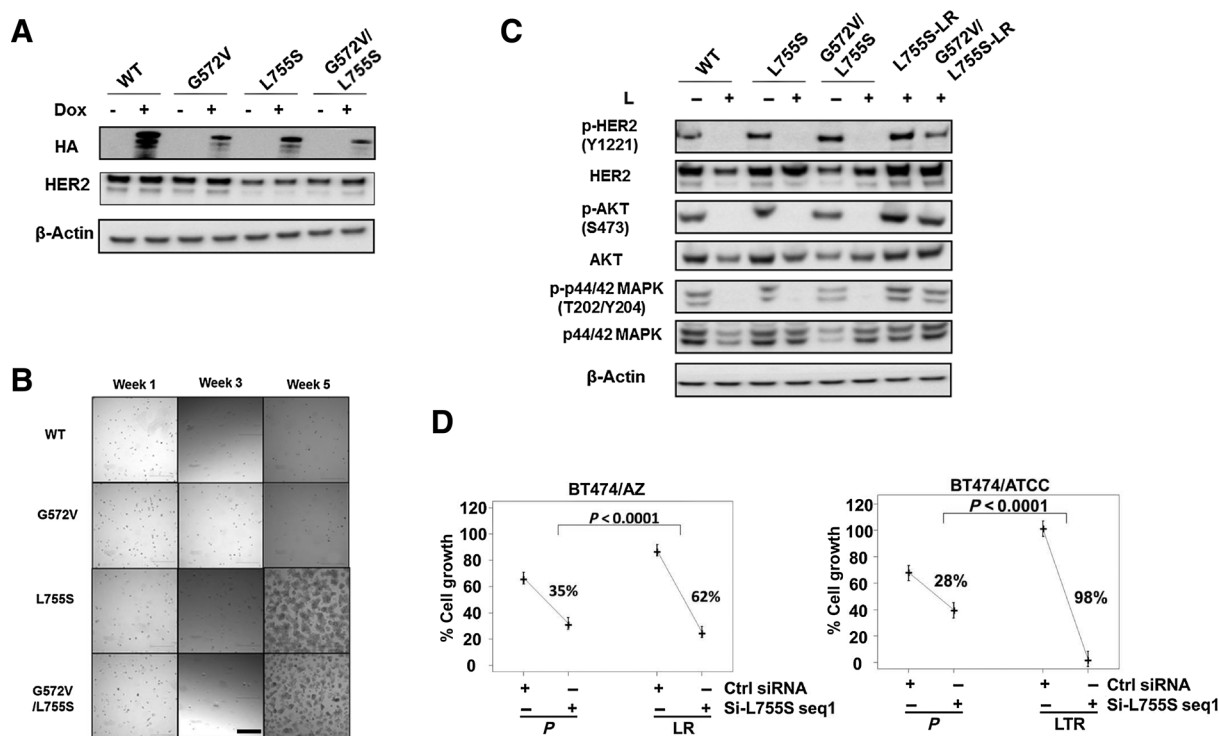
Figure 2.
The *HER2*L755S mutation but not the G572V mutation is the driver of acquired resistance in the two BT474 LR/LTR derivatives with HER2 reactivation. **A,** Doxycycline (Dox)-inducible ectopic expression of C-terminal HA-tagged WT and mutant HER2 constructs was validated by Western blot analysis. **B,** WT-, G572V-, L755S-, and G572V/L755S-HER2–expressing BT474/AZ-P cells were selected with doxycycline + lapatinib (L) for 5 weeks. Pictures were taken at 4× magnification using an Olympus IX70 microscope with a RETIGA 1300R Fast 1394 camera and analyzed with Image-pro plus software (version 5.0). Scale bar, 50 μm. **C,** WT-, G572V-, L755S-, and G572V/L755S-HER2–expressing BT474/AZ-P cells, were treated with or without 1 μmol/L lapatinib (L) for 6 hours followed by Western blot analysis. L755S- and G572V/L755S-HER2–expressing BT474/AZ-P cells, which survived the doxycycline + lapatinib selection for >5 weeks (L755S-LR and G572V/L755S-LR), were analyzed by Western blot analysis for HER2 and downstream signaling. **D,** BT474 parental and HER2-reactivated LR/LTR cells were transfected with siRNA (seq1) targeting the *HER2*L755S mutant. Culture medium was replaced the next day with regular medium or drug-containing medium, and replaced again at 4 days. Cell growth was assessed at 6 days by methylene blue assay. Relative percent (%) growth was normalized to mock transfection. Statistical analyses were performed for AZ and ATCC separately. Model-estimated group means and 95% confidence limits were plotted combining two independent experiments.

2B). No additive survival benefit was observed comparing the G572/L755S *HER2*–expressing cells versus the L755S *HER2*-expressing cells. In these surviving lapatinib-resistant L755S *HER2*- and G572/L755S *HER2*–transduced cells, HER2 and downstream signaling was reactivated in the presence of lapatinib (Fig. 2C). This suggests that the *HER2*L755S mutation can induce lapatinib resistance in BT474/AZ-P cells and that the *HER2*G572V mutation can neither induce resistance nor enhance resistance driven by the *HER2*L755S mutation in this model system. Exogenous overexpression of the *HER2*L755S but not WT HER2 also conferred lapatinib resistance in two additional HER2⁺ breast cancer models, SK-BR-3 and AU565 (Supplementary Fig. S2). This suggests that the *HER2*L755S mutation can confer lapatinib resistance in HER2⁺ breast cancer models irrespective of their genetic background.

To confirm that the *HER2*L755S mutation is the driver of acquired resistance in the BT474/AZ-LR and BT474/ATCC-LTR cells, several siRNAs specifically targeting the *HER2*L755S mutation were designed (Supplementary Methods) and applied to the resistant derivatives and their parental lines with two siRNAs tested effective and specific. Mutant-specific qPCR

assays (Supplementary Fig. S3A) confirmed effective and selective knockdown of the mutation in the two resistant lines (Supplementary Fig. S3B). The mutant-specific siRNA seq1 significantly inhibited growth of the two resistant lines (Fig. 2D). Modest growth inhibition was observed in the BT474 parental cells by mutant-specific siRNA, which could be attributed to the partial target effect of mutant-specific siRNA on total HER2 (Fig. 2D; Supplementary Fig. S3B). Growth inhibition of the two resistant lines by mutant-specific siRNA, however, was markedly greater than that of their parental lines (Fig. 2D). To further confirm, we tested a second *HER2*L755S mutant-specific siRNA, seq2 (Supplementary Fig. S3C), which showed similar substantially higher growth inhibition in the BT474/AZ-LR cells over BT474/AZ-P cells (Supplementary Fig. S4A). Furthermore, Western blot analysis following *HER2*L755S knockdown using siRNA seq2 showed a selective inhibition of phospho-HER2 as well as phospho-AKT levels in BT474/AZ-LR cells as opposed to BT474/AZ-P cells (Supplementary Fig. S4B). This suggests that the HER2 signaling reactivation observed in the LR derivatives is indeed driven by *HER2*L755S. Collectively, the results suggest that the *HER2*L755S mutation is the driver of acquired L and LT

resistance in BT474/AZ-LR and BT474/ATCC-LTR lines, respectively, with HER2 reactivation.

Next, we asked whether the *HER2*L755S mutation could also confer resistance to more potent and commonly used anti-HER2 drug regimens. As shown in Supplementary Fig. S5, we found that the *HER2*L755S mutation conferred complete resistance not only to the dual regimen lapatinib + trastuzumab but also trastuzumab + pertuzumab and partial resistance to the antibody–drug conjugate trastuzumab emtansine (T-DM1), both when expressed endogenously in the BT474/AZ-LR cell line (Supplementary Fig. S5A) as well as when expressed exogenously by doxycycline induction in the BT474/AZ-P cells (Supplementary Fig. S5B).

Irreversible HER1/2 inhibitors overcome acquired resistance to lapatinib-containing HER2-targeted therapy conferred by the *HER2*L755S mutation in the BT474 models *in vitro*

It has been suggested by structural modeling that the *HER2*L755S mutation disrupts the inactive conformation of the kinase domain, which is required for lapatinib binding (24, 25). The HER1/2–irreversible TKIs such as afatinib and neratinib were designed to covalently bind and irreversibly block enzymatically active HER1/2 receptors (45). Afatinib has been shown to effectively inhibit Ba/F3 cells ectopically expressing *HER2*L755S (24, 25), and neratinib has shown great efficacy in inhibiting growth of MCF10A cells ectopically expressing *HER2*L755S (20). Therefore, we hypothesized that the irreversible HER1/2 inhibitors can overcome acquired resistance to lapatinib-containing HER2-targeted therapy in our HER2-amplified BT474-resistant lines endogenously harboring the *HER2*L755S mutation. Cell growth assays showed that the BT474/AZ-LR and BT474/ATCC-LTR cells, which are highly resistant to lapatinib treatment (IC$_{50} \geq$ 3 µmol/L), can be effectively inhibited by afatinib and neratinib in a dose-dependent manner (IC$_{50} <$ 25 nmol/L; Fig. 3A). Furthermore, Western blot analyses confirmed that reactivated HER2 signaling in the two resistant lines was significantly inhibited by 6 hours of 50 nmol/L afatinib or neratinib treatment, which is lower than the clinically relevant concentrations of these agents (100 nmol/L; Fig. 3B). Importantly, in the BT474/AZ model, the activity of afatinib was observed only in the LR cells that were dependent on active HER2 signaling for resistant growth, and not in the LTR cells where HER signaling remained inhibited under anti-HER2 treatment (Supplementary Fig. S6; ref. 10).

Afatinib overcomes acquired resistance to HER2-targeted therapy in the BT474/AZ-LR xenografts *in vivo*

To investigate whether afatinib can serve as an effective treatment to overcome resistance to HER2-targeted therapy induced by the *HER2*L755S mutation in *HER2*-amplified breast cancer, we tested its effect *in vivo* using the BT474/AZ-LR line grown as xenografts. Mice bearing BT474/AZ-LR xenografts at approximately 150 mm^3 that were developed in the presence of E2-supplemented lapatinib treatment were randomized to E2 + lapatinib and E2 + afatinib treatment groups (Fig. 4A). Tumor progression was completely inhibited in the E2 + afatinib arm compared with E2 + lapatinib arm (P = 0.0038; Fig. 4B). Harvested on day 16 postrandomization, the E2 + afatinib tumors were markedly smaller compared with the E2 + lapatinib tumors (Fig. 4B; Supplementary Fig. S7).

We have previously shown that in both preclinical and clinical HER2+/ER+ tumors, blockade of both HER2 and ER signaling is required for long-term tumor regression to be achieved (10, 12).

Therefore, endocrine deprivation (ED) treatment was added to the experiment to mimic the clinical scenario of treating ER+/HER2+ breast cancer patients. Mice bearing the BT474/AZ-LR xenografts at an average size of approximately 350 mm^3 that had developed in the presence of E2 + lapatinib were randomized to ED + Veh, ED + lapatinib, and ED + afatinib arms. The tumors continued to grow in both ED and ED + lapatinib groups but regressed in the ED + afatinib group (Supplementary Fig. S8A), except one mouse in the ED + afatinib group that showed *de novo* resistance (Supplementary Fig. S8B) and so has been excluded from the analysis of the growth curves. With ED treatment, median time to tumor progression (TTP) was numerically, though not significantly, increased in the ED + lapatinib group compared with the ED + Veh group (33.7 and 8.5 days, respectively, P = 0.0928), and not yet achieved in the ED + afatinib group at day 85 (P = 0.0014; Fig. 4C; Supplementary Table S4). Only two mice of the ED + afatinib group progressed with the treatment (Supplementary Fig. S8B and S8C). Conversely, median time to tumor regression (TTR) was not achieved in the ED + Veh and ED + lapatinib groups at day 85 (Supplementary Table S4). Compared with ED + Veh group, response (regression) rate was significantly improved in the ED + afatinib group (P = 0.0094) but not the ED + lapatinib group (Supplementary Table S4). Importantly, complete regression (CR) was achieved in 5 of 12 of the mice in the ED + afatinib arm after 71 days of treatment, and no tumor regrowth was observed after removal of afatinib and resupplementing E2 pellets for >100 days (Supplementary Fig. S8D). We next examined the effect of afatinib on HER2 and key downstream signaling in the HER2-reactivated BT474/AZ-LR xenografts. Levels of p-HER2/p-AKT/p-MAPK were immunohistochemically assessed, and p-HER2/p-AKT/p-MAPK levels were significantly reduced in tumors which switched to afatinib treatment compared with those continued with lapatinib treatment in both E2 and ED settings (Fig. 4D). In the ED + afatinib arm, we focused on analyzing signaling changes within the 10 of 12 mice that were not resistant to the therapy.

Discussion

Acquired resistance to HER2-targeted therapies in HER2+ breast cancer can occur through reactivating the HER pathway or switching to alternative survival pathways (10, 15). In this study, we identified HER2 reactivation by acquisition of the *HER2*L755S mutation as a mechanism of acquired resistance to HER2-targeted therapy in our two HER2+ BT474 cell line models. In previous preclinical studies, forced expression of this mutation in HER2-negative cells was found to result in lapatinib resistance (20, 24, 25), and *HER2*-activating mutations were reported as a mechanism other than *HER2* amplification to drive breast tumor growth (20). Here we report on the novel observation that in *HER2*-amplified breast cancer cells the *HER2* mutation (L755S) can be gained during HER2-targeted therapy, and that this mutation may result in reactivation of the HER signaling network and induction of resistance to potent lapatinib-containing anti-HER2 therapy models. Interestingly, Zabransky and colleagues (46) reported in preclinical *in vitro* and mouse models that *HER2* missense mutations as single copies may require additional oncogenic input to induce tumorigenesis and may not by themselves predict response to HER2-targeted therapies. Our study, however, demonstrates that the HER2+ BT474/AZ-LR xenografts endogenously expressing the *HER2*L755S mutation

Xu et al.
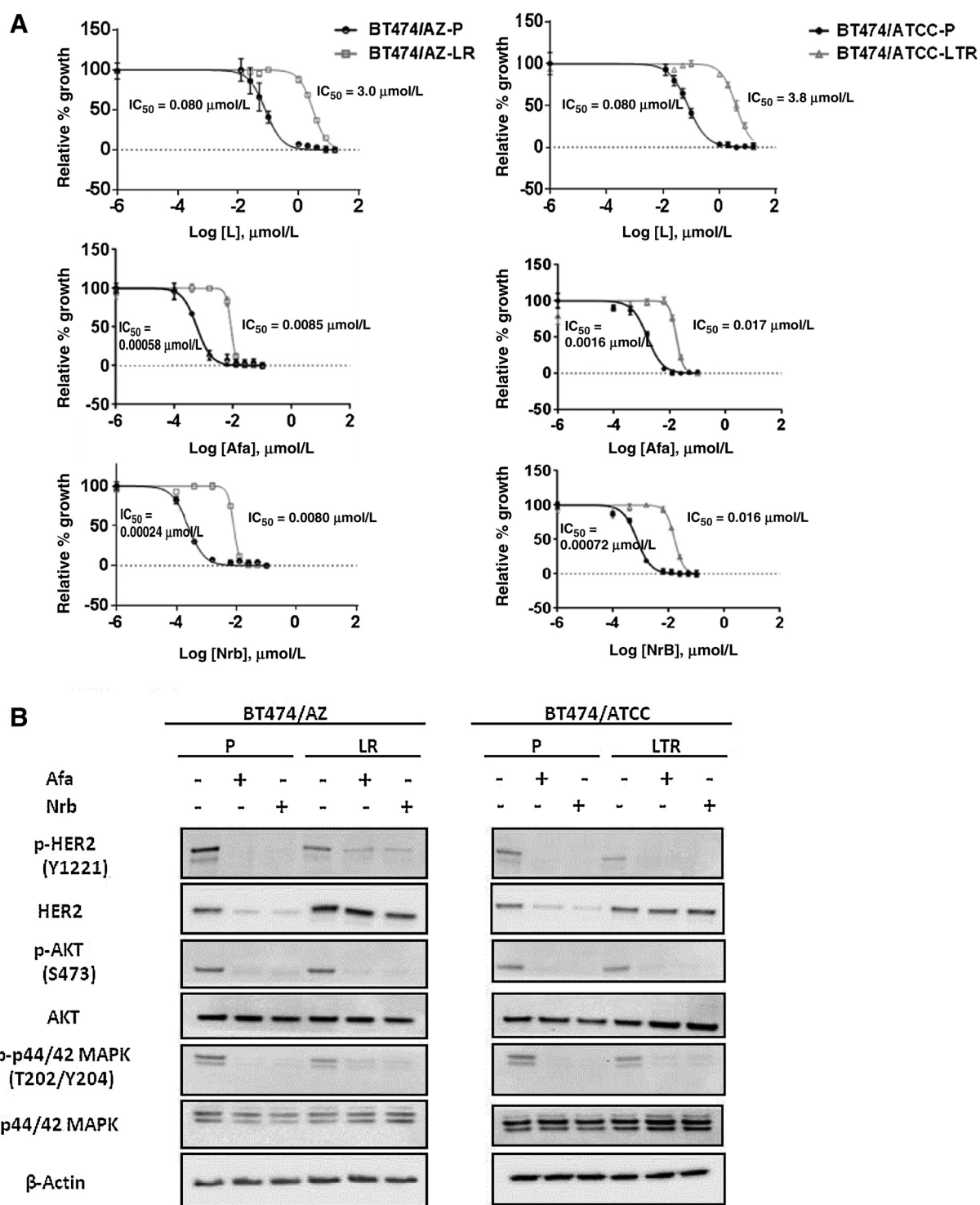
Figure 3.
The irreversible HER1/2 inhibitors overcome acquired resistance to HER2-targeted therapy conferred by the *HER2*L755S mutation in BT474 models *in vitro*.
A, Responses of BT474/AZ-LR and BT474/ATCC-LTR lines and their relative parental lines (BT474/AZ-P and BT474/ATCC-P) to lapatinib (L), afatinib (Afa), and neratinib (Nrb) were measured by cell growth assay. Data were analyzed by GraphPad Prism (version 6.05) to generate drug response curves and relative IC$_{50}$ values using the log (inhibitor) versus response-variable slope model (bars, SEM) with normalization of data defining the biggest number in each dataset as 100% and the smallest number in the same dataset as 0%. **B,** BT474/AZ-P, BT474/AZ-LR, BT474/ATCC-P, and BT474/ATCC-LTR lines were treated with or without 6 hours of 50 nmol/L afatinib or neratinib followed by Western blot analysis.
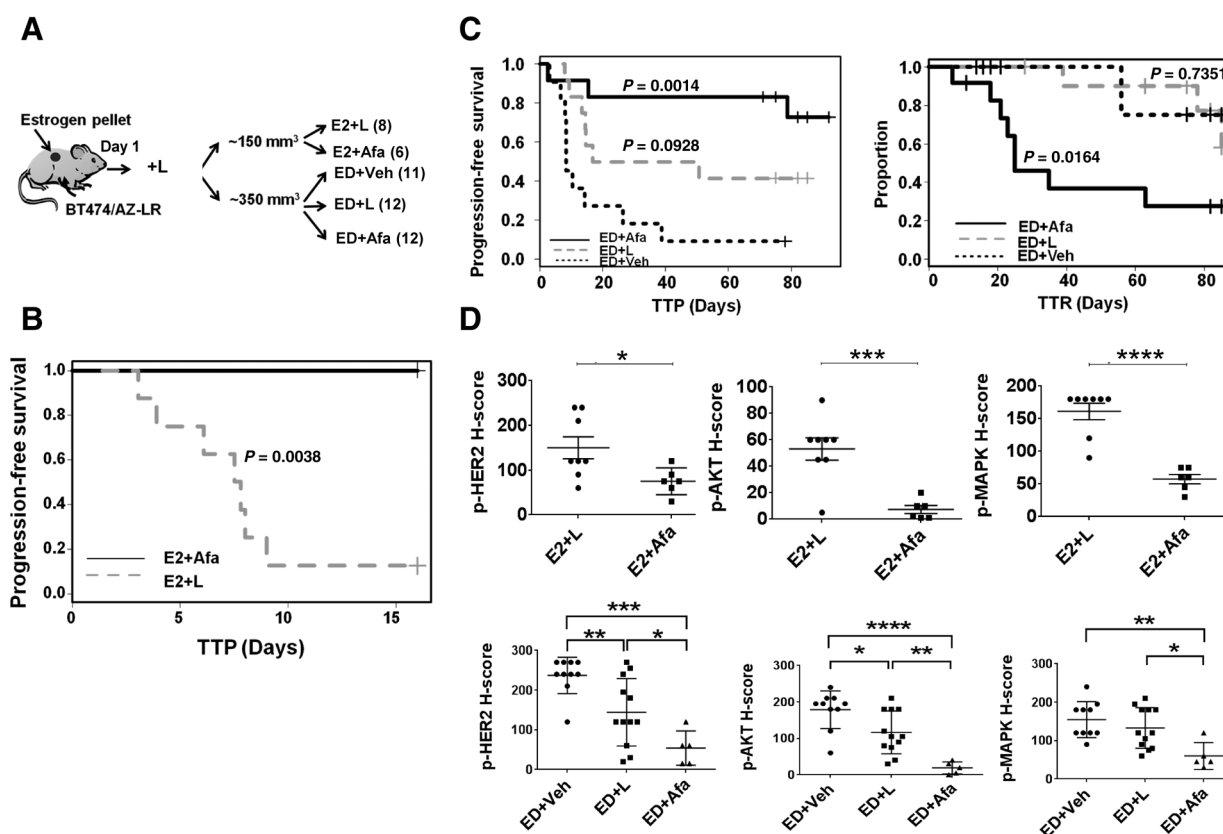
Figure 4.
Afatinib (Afa) effectively overcomes acquired resistance in the BT474/AZ-LR xenografts. **A,** Mice prepped with estrogen (E2) pellets were injected with 5×10^6 BT474/AZ-LR cells and treated with lapatinib (L) until randomization to 5 groups: E2 + lapatinib, E2 + afatinib, ED + Veh, ED + lapatinib, and ED + afatinib (see Materials and Methods for details). **B,** Kaplan–Meier analyses of progression-free survival within 16 days of treatment of E2 + afatinib or E2 + lapatinib. Tumor progression was defined as tumor size tripling since randomization. TTP, time to tumor progression. **C,** Kaplan–Meier analyses of progression-free survival and tumor regression (graph showing change of proportion of nonregressing tumors) within 85 days of ED + Veh, ED + lapatinib, or ED + afatinib treatment. Tumor regression was defined as tumor size halving since the day of randomization. TTR, time to tumor regression. **D,** p-HER2 (Y1221), p-AKT (S473), and p-p44/42 MAPK (T202/Y204) levels of xenografts in each treatment arm were assessed by IHC and scored as H-score by a pathologist. Two tumors (Supplementary Fig. S8B and S8C) that were resistant to the ED + afatinib regimen were not included in the analysis. *, $P < 0.05$; **, $P < 0.01$; ***, $P < 0.001$.

are tumorigenic even under lapatinib treatment, and that this mutation can restore HER2 activity and cause resistance to therapy in HER2+ breast cancer.

As we have identified the *HER2*L755S mutation as the mechanism of acquired resistance in two of the BT474 derivatives resistant to lapatinib-containing regimens, we postulated that the resistant clone could have originated from clonal selection of a preexisting subclone present prior to HER2-targeted therapy, or it could have appeared *de novo* during the course of treatment. Although direct evidence of the presence of the *HER2*L755S mutation in the BT474/AZ-P and BT474/ATCC-P cells could not be obtained through digital droplet PCR analysis, we cannot rule out the possibility that the methods employed here lacked the sensitivity to detect a minor resistant subclone (<0.01%) in the parental lines.

It is worth mentioning that in the BT474/AZ-LR line, we found the *HER2* L755S mutation was clonally present in all cells of the resistant line based on bioinformatics inferences made using ABSOLUTE and on single-cell cloning. Importantly, however, this mutation was expressed at approximately 30% of the alleles at the transcriptomic level and displayed a variant allelic fraction of

approximately 30%. Thus, in the case of simultaneous *HER2* amplification and L755S mutation, the most parsimonious explanation for these findings is that the *HER2*L755S mutation likely developed later in the evolution of the cell line.

The clinical relevance of the *HER2* mutations stems from their presence in intrinsic/posttreatment clinical HER2+ breast cancers. To date, HER2 missense mutations have been reported by TCGA in approximately 3% of breast cancer patients with primary HER2+ tumors (results based on cBioPortal; refs. 22, 23). A similar rate of *HER2* mutations (2.3%) was also recently reported in the study by Zuo and colleagues in a large cohort of 910 HER2+ primary breast tumors (47). The role of *HER2* mutations in acquired resistance to HER2-targeted therapies in HER2+ breast cancer, however, still remains unclear. Importantly, the *HER2*L755S mutation, which is the most common *HER2* mutation in breast cancer, has been reported in 3 of 40 (7.59%) metastatic patients who had received prior trastuzumab treatment in the adjuvant setting (48). In addition, the study by Zuo and colleagues analyzed 18 pairs of primary and metastatic lesions, 16 of which had received 1 year of adjuvant trastuzumab treatment, and observed that the drug-resistant *HER2*L755S mutation was

present in 3 of 18 metastatic lesions but not in any of the paired primary tumors. Interestingly, a second close mutation, HER2K753E, which also confers preclinical resistance to lapatinib and trastuzumab, also emerged in 2 of these 18 metastatic lesions (47). This suggests that these two HER2 mutations are associated with clinically acquired resistance to T. Through targeted sequencing of 76 HER2$^+$ primary invasive carcinomas, Boulbes and colleagues (49) identified 12 missense mutations in the HER family kinase domain, including 3 in the HER2 kinase domain (but excluding the L755S variant) that are associated with aggressiveness of the tumor and resistance to trastuzumab-based therapy in the metastatic setting. Overall, these studies suggest the occurrence and role of the HER2L755S mutation, amongst other mutations, in intrinsic and acquired HER2 therapy resistance in breast cancer.

Importantly, we have demonstrated that dual HER1/2–irreversible kinase inhibitors such as afatinib and neratinib can effectively overcome acquired resistance to HER2-targeted therapy in breast cancer cells harboring simultaneous HER2 amplification and L755S somatic mutation. In our ER$^+$/HER2$^+$ BT474 models, we have shown that reactivated HER2 and downstream signaling (such as AKT and MAPK) by the HER2L755S mutation can be significantly inhibited by low and clinically relevant concentrations of these inhibitors in vitro and in vivo. These cells, in vitro, were resistant not only to the dual regimen lapatinib + trastuzumab but also trastuzumab + pertuzumab and were less sensitive to T-DM1. We have further shown that afatinib combined with endocrine therapy can achieve stable complete tumor regression in the ER$^+$/HER2$^+$ BT474/AZ-LR xenografts harboring the L755S mutation. This suggests that treating ER$^+$/HER2$^+$ breast cancer patients harboring the HER2L755S mutation with irreversible HER1/2 inhibitors such as afatinib or neratinib instead of lapatinib might improve clinical outcome. The ExteNet trial has demonstrated a small additional benefit from one year of neratinib after completion of adjuvant trastuzumab in high risk HER2$^+$ breast cancers (50). Whether this added benefit is related to the presence of HER2 mutations remains to be determined. The therapeutic potential of the HER1/2–irreversible TKIs in HER2-negative breast cancer patients, where HER2 signaling is activated by HER2 mutations, is being investigated by Ma and colleagues (NCT01670877; ref. 51). The results of that study so far indicate that in 16 heavily pretreated HER2$^-$ metastatic breast cancer patients (14/16 with known activating HER2 mutations, 2/16 with HER2 mutations of unknown significance), single-agent neratinib treatment resulted in a 36% clinical benefit rate in the patients whose tumors harbored known activating HER2 mutations. Yet the majority of the patients with those HER2 mutations did not benefit from neratinib treatment alone. A recent preclinical study in ER$^+$ MCF7 cells expressing HER2 kinase domain mutations (52), as well as early results from an additional clinical trial investigating the efficacy of neratinib + fulvestrant in ER$^+$ metastatic breast cancer patients with HER2 mutations (SUMMIT, NCT01953926; ref. 53), further support the notion that a simultaneous inhibition of ER (fulvestrant) and the mutant HER2 by irreversible TKIs is needed. However, a significant portion of patients did not benefit even with the combination of neratinib + fulvestrant while other patients developed acquired resistance. Interestingly, we observed acquired resistance to ED + afatinib treatment in our BT474/AZ-LR xenografts (Supplementary Fig. S8C). It is important to understand the mechanism of intrinsic and acquired resistance to afatinib and neratinib in

breast tumors expressing WT or mutant HER2. More afatinib/neratinib-resistant models are currently under development through in vitro and in vivo approaches to understand the involvement of additional acquired HER2 mutations, as has been recently suggested (54), as well as the role of additional pathways.

To summarize, here we have identified HER2 reactivation through acquisition of the HER2L755S mutation as a mechanism of acquired resistance to lapatinib-containing HER2-targeted therapy in preclinical HER2$^+$ breast cancer models. This resistance can be overcome by treating the tumors harboring the L755S mutation with irreversible HER1/2 inhibitors. Our findings warrant further studies investigating the role of this mutation and other HER2 mutations in acquired resistance in HER2$^+$ breast cancer through sequencing analyses of larger numbers of tumor pairs pre- and post HER2-targeted treatment in the clinical setting. Likewise, additional clinical trials are needed to identify the subset of breast cancer patients whose tumors harbor HER2 mutations who might benefit from irreversible HER1/2 TKIs such as neratinib and afatinib.

Disclosure of Potential Conflicts of Interest

J.W. Gray holds ownership interest (including patents) in Abbott Laboratories. R. Schiff reports receiving commercial research grants from AstraZeneca and Gilead Sciences and is a consultant/advisory board member for Eli Lilly and Company. No potential conflicts of interest were disclosed by the other authors.

Disclaimer

The content is solely the responsibility of the authors and does not necessarily represent the official views of the NIH.

Authors' Contributions

Conception and design: X. Xu, H. Hu, B.H. Park, M.F. Rimawi, B. Weigelt, J.S. Reis-Filho, C.K. Osborne, R. Schiff
Development of methodology: X. Xu, A. Nardone, C.K.Y. Ng, I. Waters, B. Weigelt, C.K. Osborne, R. Schiff
Acquisition of data (provided animals, acquired and managed patients, provided facilities, etc.): X. Xu, C. De Angelis, A. Nardone, H. Hu, L. Qin, J. Veeraraghavan, V. Sethunath, M. Shea, T. Mitchell, I. Waters, D.J. Zabransky, C. Gutierrez, C. Nagi, F.C. Geyer, B.H. Park, M.F. Rimawi, C.K. Osborne, R. Schiff
Analysis and interpretation of data (e.g., statistical analysis, biostatistics, computational analysis): X. Xu, C. De Angelis, K.A. Burke, A. Nardone, J. Veeraraghavan, V. Sethunath, L.M. Heiser, C.K.Y. Ng, E. Chen, A. Renwick, T. Wang, M. Shea, I. Waters, B.H. Park, C. Shaw, S.G. Hilsenbeck, J.S. Reis-Filho, C.K. Osborne, R. Schiff
Writing, review, and/or revision of the manuscript: X. Xu, C. De Angelis, K.A. Burke, J. Veeraraghavan, V. Sethunath, L.M. Heiser, C.K.Y. Ng, E. Chen, T. Wang, T. Mitchell, I. Waters, D.J. Zabransky, C. Nagi, G.C. Chamness, B.H. Park, S.G. Hilsenbeck, M.F. Rimawi, J.W. Gray, B. Weigelt, J.S. Reis-Filho, C.K. Osborne, R. Schiff
Administrative, technical, or material support (i.e., reporting or organizing data, constructing databases): X. Xu, A. Nardone, E. Chen, S. Nanda, M. Rajendran, K.L. Scott, R. Schiff
Study supervision: X. Xu, J.S. Reis-Filho, C.K. Osborne, R. Schiff
Other (helping with cell lines): S. Nanda

References

1. Slamon DJ, Clark GM, Wong SG, Levin WJ, Ullrich A, McGuire WL. Human breast cancer: correlation of relapse and survival with amplification of the HER-2/neu oncogene. Science 1987;235:177–82.
2. Geyer CE, Forster J, Lindquist D, Chan S, Romieu CG, Pienkowski T, et al. Lapatinib plus capecitabine for HER2-positive advanced breast cancer. N Engl J Med 2006;355:2733–43.
3. Romond EH, Perez EA, Bryant J, Suman VJ, Geyer CE Jr, Davidson NE, et al. Trastuzumab plus adjuvant chemotherapy for operable HER2-positive breast cancer. N Engl J Med 2005;353:1673–84.
4. Slamon DJ, Leyland-Jones B, Shak S, Fuchs H, Paton V, Bajamonde A, et al. Use of chemotherapy plus a monoclonal antibody against HER2 for metastatic breast cancer that overexpresses HER2. N Engl J Med 2001; 344:783–92.
5. Smith I, Procter M, Gelber RD, Guillaume S, Feyereislova A, Dowsett M, et al. 2-year follow-up of trastuzumab after adjuvant chemotherapy in HER2-positive breast cancer: a randomised controlled trial. Lancet 2007; 369:29–36.
6. Gianni L, Pienkowski T, Im YH, Roman L, Tseng LM, Liu MC, et al. Efficacy and safety of neoadjuvant pertuzumab and trastuzumab in women with locally advanced, inflammatory, or early HER2-positive breast cancer (NeoSphere): a randomised multicentre, open-label, phase 2 trial. Lancet Oncol 2012;13:25–32.
7. Verma S, Miles D, Gianni L, Krop IE, Welslau M, Baselga J, et al. Trastuzumab emtansine for HER2-positive advanced breast cancer. N Engl J Med 2012;367:1783–91.
8. Arpino G, Gutierrez C, Weiss H, Rimawi M, Massarweh S, Bharwani L, et al. Treatment of human epidermal growth factor receptor 2-overexpressing breast cancer xenografts with multiagent HER-targeted therapy. J Natl Cancer Inst 2007;99:694–705.
9. Rimawi MF, Wiechmann LS, Wang YC, Huang C, Migliaccio I, Wu MF, et al. Reduced dose and intermittent treatment with lapatinib and trastuzumab for potent blockade of the HER pathway in HER2/neu-overexpressing breast tumor xenografts. Clin Cancer Res 2011;17:1351–61.
10. Wang YC, Morrison G, Gillihan R, Guo J, Ward RM, Fu X, et al. Different mechanisms for resistance to trastuzumab versus lapatinib in HER2-positive breast cancers–role of estrogen receptor and HER2 reactivation. Breast Cancer Res 2011;13:R121.
11. Baselga J, Bradbury I, Eidtmann H, Di Cosimo S, de Azambuja E, Aura C, et al. Lapatinib with trastuzumab for HER2-positive early breast cancer (NeoALTTO): a randomised, open-label, multicentre, phase 3 trial. Lancet 2012;379:633–40.
12. Rimawi MF, Mayer IA, Forero A, Nanda R, Goetz MP, Rodriguez AA, et al. Multicenter phase II study of neoadjuvant lapatinib and trastuzumab with hormonal therapy and without chemotherapy in patients with human epidermal growth factor receptor 2-overexpressing breast cancer: TBCRC 006. J Clin Oncol 2013;31:1726–31.
13. Blackwell KL, Pegram MD, Tan-Chiu E, Schwartzberg LS, Arbushites MC, Maltzman JD, et al. Single-agent lapatinib for HER2-overexpressing advanced or metastatic breast cancer that progressed on first- or second-line trastuzumab-containing regimens. Ann Oncol 2009;20:1026–31.
14. Nahta R, Yu D, Hung MC, Hortobagyi GN, Esteva FJ. Mechanisms of disease: understanding resistance to HER2-targeted therapy in human breast cancer. Nat Clin Pract Oncol 2006;3:269–80.
15. Rimawi MF, Schiff R, Osborne CK. Targeting HER2 for the treatment of breast cancer. Annu Rev Med 2015;66:111–28.
16. Berns K, Horlings HM, Hennessy BT, Madiredjo M, Hijmans EM, Beelen K, et al. A functional genetic approach identifies the PI3K pathway as a major determinant of trastuzumab resistance in breast cancer. Cancer Cell 2007; 12:395–402.
17. Eichhorn PJ, Gili M, Scaltriti M, Serra V, Guzman M, Nijkamp W, et al. Phosphatidylinositol 3-kinase hyperactivation results in lapatinib resistance that is reversed by the mTOR/phosphatidylinositol 3-kinase inhibitor NVP-BEZ235. Cancer Res 2008;68:9221–30.
18. Contreras A, Herrera S, Wang T, Mayer I, Forero A, Nanda R, et al. PIK3CA mutations and/or low PTEN predict resistance to combined anti-HER2 therapy with lapatinib and trastuzumab and without chemotherapy in TBCRC006, a neoadjuvant trial of HER2-positive breast cancer patients [abstract]. In: Proceedings of the San Antonio Breast Cancer Symposium; Dec 10–14; San Antonio, TX. Philadeplhia (PA): AACR; 2013. Abstract nr PD1-2.
19. Huang C, Park CC, Hilsenbeck SG, Ward R, Rimawi MF, Wang YC, et al. β1 integrin mediates an alternative survival pathway in breast cancer cells resistant to lapatinib. Breast Cancer Res 2011;13:R84.
20. Bose R, Kavuri SM, Searleman AC, Shen W, Shen D, Koboldt DC, et al. Activating HER2 mutations in HER2 gene amplification negative breast cancer. Cancer Discov 2013;3:224–37.
21. Ferrari A, Vincent-Salomon A, Pivot X, Sertier AS, Thomas E, Tonon L, et al. A whole-genome sequence and transcriptome perspective on HER2-positive breast cancers. Nat Commun 2016;7:12222.
22. Cerami E, Gao J, Dogrusoz U, Gross BE, Sumer SO, Aksoy BA, et al. The cBio cancer genomics portal: an open platform for exploring multidimensional cancer genomics data. Cancer Discov 2012;2:401–4.
23. Gao J, Aksoy BA, Dogrusoz U, Dresdner G, Gross B, Sumer SO, et al. Integrative analysis of complex cancer genomics and clinical profiles using the cBioPortal. Sci Signal 2013;6:pl1.
24. Trowe T, Boukouvala S, Calkins K, Cutler RE Jr, Fong R, Funke R, et al. EXEL-7647 inhibits mutant forms of ErbB2 associated with lapatinib resistance and neoplastic transformation. Clin Cancer Res 2008;14: 2465–75.
25. Kancha RK, von Bubnoff N, Bartosch N, Peschel C, Engh RA, Duyster J. Differential sensitivity of ERBB2 kinase domain mutations towards lapatinib. PLoS One 2011;6:e26760.
26. Li H, Durbin R. Fast and accurate short read alignment with Burrows-Wheeler transform. Bioinformatics 2009;25:1754–60.
27. McKenna A, Hanna M, Banks E, Sivachenko A, Cibulskis K, Kernytsky A, et al. The Genome Analysis Toolkit: a MapReduce framework for analyzing next-generation DNA sequencing data. Genome Res 2010;20: 1297–303.
28. Cibulskis K, Lawrence MS, Carter SL, Sivachenko A, Jaffe D, Sougnez C, et al. Sensitive detection of somatic point mutations in impure and heterogeneous cancer samples. Nat Biotechnol 2013;31:213–9.
29. Koboldt DC, Zhang Q, Larson DE, Shen D, McLellan MD, Lin L, et al. VarScan 2: somatic mutation and copy number alteration discovery in cancer by exome sequencing. Genome Res 2012;22:568–76.
30. Saunders CT, Wong WS, Swamy S, Becq J, Murray LJ, Cheetham RK. Strelka: accurate somatic small-variant calling from sequenced tumor-normal sample pairs. Bioinformatics 2012;28:1811–7.
31. De Mattos-Arruda L, Weigelt B, Cortes J, Won HH, Ng CK, Nuciforo P, et al. Capturing intra-tumor genetic heterogeneity by de novo mutation profiling of circulating cell-free tumor DNA: a proof-of-principle. Ann Oncol 2014;25:1729–35.
32. Carter SL, Cibulskis K, Helman E, McKenna A, Shen H, Zack T, et al. Absolute quantification of somatic DNA alterations in human cancer. Nat Biotechnol 2012;30:413–21.

Xu et al.

33. Van Loo P, Nordgard SH, Lingjaerde OC, Russnes HG, Rye IH, Sun W, et al. Allele-specific copy number analysis of tumors. Proc Natl Acad Sci U S A 2010;107:16910–5.

34. Trapnell C, Pachter L, Salzberg SL. TopHat: discovering splice junctions with RNA-Seq. Bioinformatics 2009;25:1105–11.

35. Li H, Handsaker B, Wysoker A, Fennell T, Ruan J, Homer N, et al. The Sequence Alignment/Map format and SAMtools. Bioinformatics 2009; 25:2078–9.

36. Robinson JT, Thorvaldsdottir H, Winckler W, Guttman M, Lander ES, Getz G, et al. Integrative genomics viewer. Nat Biotechnol 2011;29:24–6.

37. Meerbrey KL, Hu G, Kessler JD, Roarty K, Li MZ, Fang JE, et al. The pINDUCER lentiviral toolkit for inducible RNA interference in vitro and in vivo. Proc Natl Acad Sci U S A 2011;108:3665–70.

38. Rexer BN, Chanthaphaychith S, Dahlman K, Arteaga CL. Direct inhibition of PI3K in combination with dual HER2 inhibitors is required for optimal antitumor activity in HER2+ breast cancer cells. Breast Cancer Res 2014;16:R9.

39. Schwarz DS, Ding H, Kennington L, Moore JT, Schelter J, Burchard J, et al. Designing siRNA that distinguish between genes that differ by a single nucleotide. PLoS Genet 2006;2:e140.

40. Dupont S, Morsut L, Aragona M, Enzo E, Giulitti S, Cordenonsi M, et al. Role of YAP/TAZ in mechanotransduction. Nature 2011;474:179–83.

41. Ariazi EA, Lewis-Wambi JS, Gill SD, Pyle JR, Ariazi JL, Kim HR, et al. Emerging principles for the development of resistance to antihormonal therapy: implications for the clinical utility of fulvestrant. J Steroid Biochem Mol Biol 2006;102:128–38.

42. Morrison G, Fu X, Shea M, Nanda S, Giuliano M, Wang T, et al. Therapeutic potential of the dual EGFR/HER2 inhibitor AZD8931 in circumventing endocrine resistance. Breast Cancer Res Treat 2014;144:263–72.

43. Scaltriti M, Verma C, Guzman M, Jimenez J, Parra JL, Pedersen K, et al. Lapatinib, a HER2 tyrosine kinase inhibitor, induces stabilization and accumulation of HER2 and potentiates trastuzumab-dependent cell cytotoxicity. Oncogene 2009;28:803–14.

44. Nahta R, Yuan LX, Du Y, Esteva FJ. Lapatinib induces apoptosis in trastuzumab-resistant breast cancer cells: effects on insulin-like growth factor I signaling. Mol Cancer Ther 2007;6:667–74.

45. Solca F, Dahl G, Zoephel A, Bader G, Sanderson M, Klein C, et al. Target binding properties and cellular activity of afatinib (BIBW 2992), an irreversible ErbB family blocker. J Pharmacol Exp Ther 2012;343:342–50.

46. Zabransky DJ, Yankaskas CL, Cochran RL, Wong HY, Croessmann S, Chu D, et al. HER2 missense mutations have distinct effects on oncogenic signaling and migration. Proc Natl Acad Sci U S A 2015;112: E6205–14.

47. Zuo WJ, Jiang YZ, Wang YJ, Xu XE, Hu X, Liu GY, et al. Dual characteristics of novel HER2 kinase domain mutations in response to HER2-targeted therapies in human breast cancer. Clin Cancer Res 2016;22: 4859–69.

48. Wagle N, Lin NU, Richardson AL, Leshchiner I, Mayer IA, Forero-Torres A, et al. Whole exome sequencing (WES) of HER2+ metastatic breast cancer (MBC) from patients with or without prior trastuzumab (T): a correlative analysis of TBCRC003. J Clin Oncol 32:5s, 2014(suppl; abstr 536).

49. Boulbes DR, Arold ST, Chauhan GB, Blachno KV, Deng N, Chang WC, et al. HER family kinase domain mutations promote tumor progression and can predict response to treatment in human breast cancer. Mol Oncol 2015;9: 586–600.

50. Chan A, Delaloge S, Holmes FA, Moy B, Iwata H, Harvey VJ, et al. Neratinib after trastuzumab-based adjuvant therapy in patients with HER2-positive breast cancer (ExteNET): a multicentre, randomised, double-blind, placebo-controlled, phase 3 trial. Lancet Oncol 2016;17:367–77.

51. Ma CX, Bose R, Gao F, Freedman RA, Pegram MD, Blackwell K, et al. Phase II trial of neratinib for HER2 mutated, non-amplified metastatic breast cancer (HER2mut MBC). J Clin Oncol 34, 2016(suppl; abstr 516).

52. Croessmann S, Cutler RE Jr, Lalani AS, Park BH, Arteaga CL. Inhibition of mutant HER2 results in synthetic lethality when combined with ER antagonists in ER+/HER2 mutant human breast cancer cells [abstract]. In: Proceedings of the 2016 San Antonio Breast Cancer Symposium; 2016 Dec 6–10; San Antonio, TX. Philadelphia (PA): AACR; 2017. Abstract nr PD2-05.

53. Hyman D, Saura C, Arteaga CL, Mayer I, Shapiro G, Loi S, et al. Neratinib + fulvestrant in ERBB2-mutant, HER2–non-amplified, estrogen receptor (ER)-positive, metastatic breast cancer (MBC): preliminary analysis from the phase II SUMMIT trial [abstract]. In: Proceedings of the 2016 San Antonio Breast Cancer Symposium; 2016 Dec 6–10; San Antonio, TX. Philadelphia (PA): AACR; 2017. Abstract nr PD2-08.

54. Hanker AB, Brewer MR, Sheehan JH, Koch JP, Sliwoski GR, Nagy R, et al. An acquired HER2 T798I gatekeeper mutation induces resistance to neratinib in a patient with HER2 mutant-driven breast cancer. Cancer Discov 2017;7:575–85.

Clinical Cancer Research

HER2 Reactivation through Acquisition of the HER2 L755S Mutation as a Mechanism of Acquired Resistance to HER2-targeted Therapy in HER2⁺ Breast Cancer

Xiaowei Xu, Carmine De Angelis, Kathleen A. Burke, et al.

Updated version	Access the most recent version of this article at: doi:10.1158/1078-0432.CCR-16-2191
Supplementary Material	Access the most recent supplemental material at: http://clincancerres.aacrjournals.org/content/suppl/2017/05/09/1078-0432.CCR-16-2191.DC1

Cited articles	This article cites 49 articles, 17 of which you can access for free at: http://clincancerres.aacrjournals.org/content/23/17/5123.full#ref-list-1
Citing articles	This article has been cited by 8 HighWire-hosted articles. Access the articles at: http://clincancerres.aacrjournals.org/content/23/17/5123.full#related-urls

E-mail alerts	Sign up to receive free email-alerts related to this article or journal.
Reprints and Subscriptions	To order reprints of this article or to subscribe to the journal, contact the AACR Publications Department at pubs@aacr.org.
Permissions	To request permission to re-use all or part of this article, use this link http://clincancerres.aacrjournals.org/content/23/17/5123. Click on "Request Permissions" which will take you to the Copyright Clearance Center's (CCC) Rightslink site.